J|A|C|S
ARTICLES

Published on Web 05/28/2009

Molecularly Tethered Amphiphiles as 3-D Supramolecular Assembly Platforms: Unlocking a Trapped Conformation

Christopher G. Clark, Jr.,*[,†,§] George A. Floudas,[‡] Young Joo Lee,[†] Robert Graf,[†] Hans W. Spiess,[†] and Klaus Müllen*[,†]

Max-Planck-Institute for Polymer Research, Ackermannweg 10, 55128 Mainz, Germany, and the Department of Physics, University of Ioannina and Biomedical Research Institute (BRI), Foundation for Research and Technology-Hellas (FORTH), Ioannina, Greece

Received February 9, 2009; E-mail: chris.clark@liquidia.com; muellen@mpip-mainz.mpg.de

Abstract: A fluorous biphasic hexa(3,5-substituted-phenyl)benzene (HPB), analogous to semifluorinated alkanes, was synthesized such that precise chemical and orthogonally directed, supramolecular placement of amphiphilic side chains at their bulk density was achieved. The grafting or tethering of incommensurate hydrocarbon and fluorocarbon chains to the rotationally flexible HPB core inextricably links intermolecular phase separation with intramolecular conformational behavior and results in rich self-assembly. The self-assembled structure was studied with polarized optical microscopy, differential scanning calorimetry, X-ray scattering, and ^{19}F magic-angle spinning solid-state NMR and found to be kinetically trapped with mixed fluorocarbon and hydrocarbon side chains, despite packing into a lattice defined by the HPB scaffold. The addition of 1% of the parent biphasic diphenylacetylene unlocks the frustrated conformation in the HPB, resulting in the formation of a thermodynamically favorable bilayer structure.

Introduction

Precise 3-D nanoscale morphological control of the solid state in the 5−10-nm range using semiflexible chains is a demanding challenge. The development of strategies for increasing the intricacy within self-assembled nanostructures outside of biology or analogous de novo examples is hindered by the ability to predict the complex competition of intra- and intermolecular interactions and surfaces formed at the molecular level. Block copolymers generate packing motifs made by the phase segregation of blocks, as dictated by the immiscibility (interaction parameter), the degree of polymerization, flexibility (conformational asymmetry), and the relative volume fraction of each polymer block.[1,2] The introduction of macromolecular branching[3,4] and variable partial specific volumes[5] into block copolymers have given rise to a host of new and rich packing motifs. While amphiphilic stars[6,7] and Janus dendritic macromolecules[8] have been synthesized previously, the grafting density has not been made near bulk density of the individual amphiphiles.

Furthermore, the incorporation of fluorocarbon units into polymers has been extensively studied because of the advantage in combining a low friction coefficient, high rigidity, extremely low surface energy, hydrophobicity, chemical inertness, and thermal resistance, which make them useful for a wide range of applications.[9] In addition, partially fluorinated compounds provide unique tools for tailoring self-assembly via the fluorophobic effect.[8,10,11] The smallest class of phase-segregating diblock copolymers is the semifluorinated alkane (SFA, Figure 1a), which with sufficient and similar block lengths are known to form fluorocarbon lamellae[12−14] through this effect.

Symmetrically tethering amphiphiles to a rigid core modulates the local repulsive and attractive interactions, providing preordered building blocks for nanostructured materials and therefore increasing control over entropic aspects of the self-assembly process. Hexaphenylbenzene[15,16] (HPB, Figure 1b), a propeller-like molecule[17] with only six rotational degrees of freedom,

† Max-Planck-Institute for Polymer Research.
‡ University of Ioannina and BRI.
§ Current address: Liquidia Technologies, P.O. Box 110085, Research Triangle Park, NC 27709; (919) 389-5132.

(1) Bates, F. S.; Fredrickson, G. H. *Annu. Rev. Phys. Chem.* **1990**, *41*, 525–557.
(2) Hadjichristidis, N.; Pispas, S.; Floudas, G. A. *Block Copolymers: Synthetic Strategies, Physical Properties, and Applications*; Wiley & Sons: Hoboken, NJ, 2003.
(3) Cho, B.-K.; Jain, A.; Gruner, S. M.; Wiesner, U. *Science* **2004**, *305*, 1598–1601.
(4) Percec, V.; Won, B. C.; Peterca, M.; Heiney, P. A. *J. Am. Chem. Soc.* **2007**, *129*, 11265–11278.
(5) Stupp, S. I.; LeBonheur, V.; Walker, K.; Li, L. S.; Huggins, K. E.; Keser, M.; Amstutz, A. *Science* **1997**, *276*, 384–389.
(6) Genson, K. L.; Hoffman, J.; Teng, J.; Zubarev, E. R.; Vaknin, D.; Tsukruk, V. V. *Langmuir* **2004**, *20*, 9044–9052.
(7) Martin, O. M.; Yu, L.; Mecozzi, S. *Chem. Commun.* **2005**, 4964–4966.
(8) Percec, V.; Imam, M. R.; Bera, T. K.; Balagurusamy, V. S. K.; Peterca, M.; Heiney, P. A. *Angew. Chem., Int. Ed.* **2005**, *44*, 4739–4745.
(9) *Modern Fluoropolymers: High Performance Polymers for Diverse Applications*; Scheirs, J., Ed.; Wiley & Sons: New York, 1997.
(10) Percec, V.; Johansson, G.; Ungar, G.; Zhou, J. *J. Am. Chem. Soc.* **1996**, *118*, 9855–9866.
(11) Xiang, M.; Li, X.; Ober, C. K.; Char, K.; Genzer, J.; Sivaniah, E.; Kramer, E. J.; Fischer, D. A. *Macromolecules* **2000**, *33*, 6106–6119.
(12) Russell, T. P.; Rabolt, J. F.; Twieg, R. J.; Siemens, R. L.; Farmer, B. L. *Macromolecules* **1986**, *19*, 1135–1143.
(13) Rabolt, J. F.; Russell, T. P.; Twieg, R. J. *Macromolecules* **1984**, *17*, 2786–2794.
(14) Höpken, J.; Möller, M. *Macromolecules* **1992**, *25*, 2482–2489.
(15) Dilthey, W.; Hurtig, G. *Chem. Ber.* **1934**, *67B*, 2004–2007.
(16) Dilthey, W.; Hurtig, G. *Chem. Ber.* **1934**, *67B*, 495–496.
(17) Bart, J. C. J. *Acta Crystallogr., Sect. B* **1968**, *24*, 1277–1287.

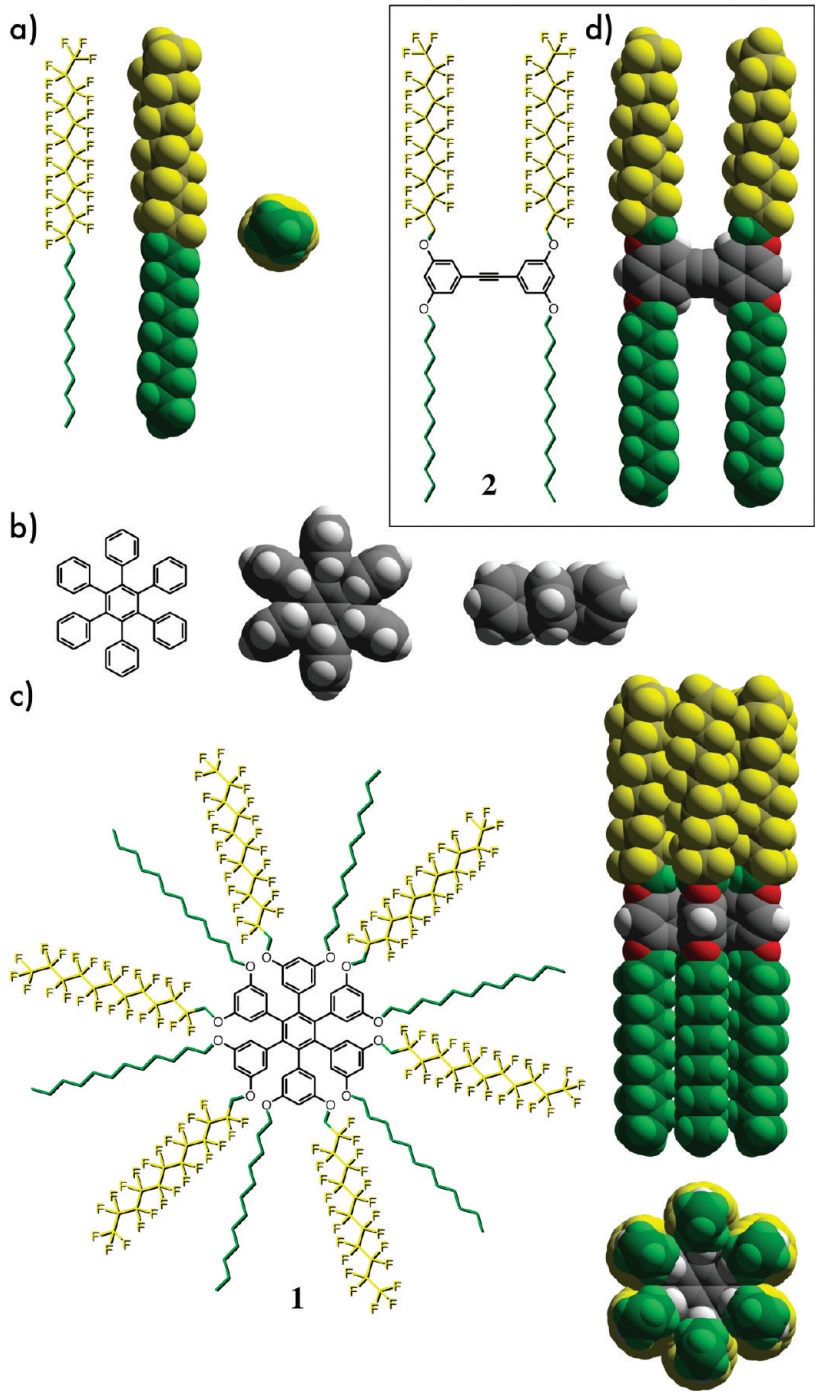

Figure 1. Constructs (chemical structure and molecular packing conformation) for tethered fluorous amphiphiles: (a) the SFA, perfluoro(dodecyl)dodecane (**F12H12**), (b) HPB, (c) the biphasic HPB, hexakis(3-(1-perfluoroundecylmethoxy)-5-dodecyloxyphenyl)benzene (**1**), and (d) the biphasic DPA, bis(3-(1-perfluoroundecylmethoxy)-5-dodecyloxyphenyl)ethyne (**2**).

gives lamellar[18−21] or columnar[22,23] packing with a variety of radial functionalities. If the phenyl rings are replaced with heteroatom containing rings, they act as highly symmetric axial receptors for metal coordination.[24−30] A hexaphenylbenzene scaffold presents the opportunity for synergistic assembly with

(18) Kobayashi, K.; Shirasaka, T.; Sato, A.; Horn, E.; Furukawa, N. *Angew. Chem., Int. Ed.* **1999**, *38*, 3483–3486.
(19) Kobayashi, K.; Shirasaka, T.; Horn, E.; Furukawa, N. *Tetrahedron Lett.* **2000**, *41*, 89–93.
(20) Kobayashi, K.; Sato, A.; Sakamoto, S.; Yamaguchi, K. *J. Am. Chem. Soc.* **2003**, *125*, 3035–3045.
(21) Kobayashi, K.; Kobayashi, N.; Ikuta, M.; Therrien, B.; Sakamoto, S.; Yamaguchi, K. *J. Org. Chem.* **2005**, *70*, 749–752.
(22) Pugh, C.; Percec, V. *J. Mater. Chem.* **1991**, *1*, 765–773.
(23) Geng, Y.; Fechtenkötter, A.; Müllen, K. *J. Mater. Chem.* **2001**, *11*, 1634–1641.
(24) Hiraoka, S.; Yi, T.; Shiro, M.; Shionoya, M. *J. Am. Chem. Soc.* **2002**, *124*, 14510–14511.
(25) Hiraoka, S.; Harano, K.; Tanaka, T.; Shiro, M.; Shionoya, M. *Angew. Chem., Int. Ed.* **2003**, *42*, 5182–5185.
(26) Hiraoka, S.; Hirata, K.; Shionoya, M. *Angew. Chem., Int. Ed.* **2004**, *43*, 3814–3818.
(27) Hiraoka, S.; Shiro, M.; Shionoya, M. *J. Am. Chem. Soc.* **2004**, *126*, 1214–1218.
(28) Hiraoka, S.; Harano, K.; Shiro, M.; Shionoya, M. *Angew. Chem., Int. Ed.* **2005**, *44*, 2727–2731.

the precise chemical grafting and supramolecular placement of block copolymer amphiphiles at or near bulk density, when oriented axially (Figure 1c). In contrast, the parent biphasic diphenylacetylene (DPA, **2**) has only two chains of each type, placed at distances greater than the sums of their van der Waals radii (Figure 1d), and as such possesses limited intramolecular interactions. In this case, the single, low internal rotational barrier of the ethyne in DPA (**2**)[31] allows the phase behavior to be determined predominantly by intermolecular interactions.

Reported herein are the synthesis and study of the solid-state assembly of per-meta-functional HPB (**1**) and DPA (**2**) molecules bearing six and two hydrocarbon and fluorocarbon chains each, respectively (Figure 1c,d), as characterized by polarized optical microscopy, differential scanning calorimetry (DSC), X-ray scattering, and ^{19}F magic-angle spinning (MAS) solid-state NMR. The HPB assembly is controlled not only by the phase separation propensities of the multiphasic components (fluorophobic effect) but also by the ability to convert between rotation (about each of the six phenylbenzene arms) conformational isomers. Thus, in contrast to the SFA case, this propeller-like molecule allows for thermodynamically unfavorable yet kinetically trapped (and long-lived) mixed conformations. It is furthermore shown that addition of a minor amount of DPA **2** to HPB **1** provides a nucleation center and in effect softens the conformational barriers for HPB rotation and gives access to the thermodynamically preferred state.

Experimental Section

Instrumentation and Methods. Microwave-heated reactions were performed in 10-mL glass vessels using a Discover 300-W microwave reactor (CEM GmbH) with a single-mode cavity equipped with an infrared temperature sensor, calibrated against DMF at ambient pressure, and an Intellivent pressure transducer. Simultaneous cooling of the reactions was made using a stream of air flow around the glass vessel at a constant flow rate with a maximum pressure differential of 50 psi. The cooling rate was adjusted to permit the application of maximum microwave power, whereby the microwave power was automatically modulated to maintain a constant reaction temperature. Solubilities of HPB **1** were evaluated in pure THF, benzene, toluene, ethyl acetate, and hexane by heating 10 mg in 50−100 uL of solvent until it dissolved and allowing the solution to cool. Gels formed in all cases. ^{1}H and ^{13}C liquid-state NMR spectra were recorded on Bruker AMX250, AC300, AMX500, and AMX700 NMR spectrometers using the residual proton of the solvent (2.05 and 6.00 ppm for acetone-d_5 and C_2HDCl_4, respectively) or the carbon signal of the deuterated solvent (29.92 and 73.78 ppm for acetone-d_6 and $C_2D_2Cl_4$, respectively) as an internal standard. ^{19}F and ^{1}H MAS NMR experiments were performed at operating frequencies of 470.53 and 500.12 MHz, respectively, on a Bruker DSX spectrometer equipped with a 2.5-mm MAS NMR probe. All ^{19}F and ^{1}H solid-state NMR spectra were acquired with spinning frequencies of 30 kHz, unless otherwise specified. The temperature was controlled with a Bruker BVT3000 and was calibrated using $Pb(NO_3)_2$ taking into account the frictional heat caused by fast spinning. ^{19}F NMR solid-state NMR chemical shift values were referenced relative to Teflon (−122.0 ppm) at room temperature. Melt-phase liquid ^{19}F NMR was acquired in coaxial NMR tubes (Wilmad LabGlass, 516-CC-5), which permit an external lock and reference signal. The liquid-state ^{19}F NMR data were cross-referenced with the solid-state NMR data using the upfield shift of bis(3,4,5-trifluorophenyl)ethyne (−157.29 ppm) in deuterated *o*-dichlorobenzene at 120 °C, which has sufficiently low volatility and whose chemical shifts are upfield of the aliphatic fluorines. With this scale, hexafluorobenzene in deuterated tetrachloroethane has an externally referenced chemical shift of −160.89 ppm. Solid-state NMR samples were placed into the rotor as a powder and annealed by cooling over 4 h from 130 to 60 °C before recording spectra. Field desorption mass spectra (FDMS) were performed with a VG-Instruments ZAB 2-SE-FDP using 8 kV accelerating voltage. MALDI-TOF mass spectra were measured using a Bruker Reflex II, calibrated against poly(ethylene glycol) (3000 g/mol). Samples for MALDI-TOF MS were prepared by ball milling with TCNQ in a ratio of 1:1000 for 40 min using an MM 2000 Retsch mixer mill. Elemental analyses of solid samples were performed by the Microanalytical Laboratory of Johannes Gutenberg University. Melting points were measured using a Büchi Melting Point Apparatus B545. Small-angle X-ray scattering (SAXS) measurements were made from macroscopically oriented (extruded at room temperature) filaments with a diameter of 0.7 mm using a 18 kW rotating-anode X-ray source with pinhole collimation and a two-dimensional detector (Siemens A102647) with 1024 × 1024 pixels. The sample-to-detector distance was set at 1.63 m. Mid-angle X-ray scattering (MAXS) and wide-angle X-ray scattering (WAXS) measurements were made using a similar setup and sample-to-detector distances of 52.8 and 7.05 cm, respectively. For the doping, DPA (**2**) and HPB (**1**) were mixed in solution using ethyl acetate, and the solvent was removed in vacuo and heated to above 130 °C until residual solvent was removed according to ^{1}H NMR. X-ray measurements of the DPA (**2**)-doped HPB (**1**) extruded fiber were performed on heating and cooling for temperatures in the range from 30 to 100 °C in steps of 10 °C. Before each measurement, the fiber was annealed for 1 h. DSC was performed with a Mettler Toledo Star differential scanning calorimeter at a rate of 10 °C/min. The sample was heated from ambient temperature to 140 °C and subsequently cooled to room temperature, and the cycle was repeated. Only the second heating run was reported.

Materials. The syntheses of 5-iodoresorcinol,[32−36] 1-perfluoroundecylmethylnonaflate,[37] and perfluoro(dodecyl)dodecane[13] (**F12H12**) are described elsewhere. All other materials were used as received from Aldrich.

Syntheses. 3,5-Bis(4-toluenesulfonyloxy)iodobenzene (3). A solution of 5-iodoresorcinol (12.22 g, 51.78 mmol) and *p*-toluenesulfonyl chloride (21.72 g, 113.91 mmol) in pyridine (115 mL) was stirred at 25 °C for 5.5 days. The residual *p*-toluenesulfonyl chloride was quenched by addition of water. The reaction mixture was extracted with diethyl ether and washed with sodium hydroxide (5%, aq) followed by hydrochloric acid (5%, aq). The solution was dried over $MgSO_4$, filtered, concentrated in vacuo, and recrystallized from methanol to yield white crystals (23.4 g, 83.0%). R_f (25% ethyl acetate/hexane) = 0.55. ^{1}H NMR (300 MHz, acetone-d_6, 20 °C): δ 2.48 (s, 6H, PhCH_3), 6.82 (t, H, $^{4}J_{HH}$ = 2.1 Hz, Ar*H*), 7.35 (d, 2H, $^{4}J_{HH}$ = 2.1 Hz, Ar*H*), 7.51 (d, 4H, $^{3}J_{HH}$ = 8.1 Hz, CH_3Ar*H*), 7.72 (d, 4H, $^{3}J_{HH}$ = 8.1 Hz, CH_3Ar*H*) ppm; ^{13}C NMR (75 MHz, acetone-d_6, 20 °C): δ 21.73, 29.92, 93.36, 117.58, 129.44, 131.19, 131.27, 132.43, 147.48, 150.81, 206.17 ppm; FDMS: *m*/*z* [ue^{-1}] 544.4 (100%), [M$^+$]; calcd, 544.0. Anal. Calcd for $C_{20}H_{17}IO_6S_2$: C, 44.13; H, 3.15; S, 11.78. Found: C, 44.06; H, 3.21; S, 11.75.

3-(4-Toluenesulfonyloxy)-5-hydroxyiodobenzene (4). A solution of potassium hydroxide (5.0 g, 89.1 mmol) in water (2.5 mL)

(29) Hiraoka, S.; Harano, K.; Shiro, M.; Ozawa, Y.; Yasuda, N.; Toriumi, K.; Shionoya, M. *Angew. Chem., Int. Ed.* **2006**, *45*, 6488–6491.
(30) Hiraoka, S.; Tanaka, T.; Shionoya, M. *J. Am. Chem. Soc.* **2006**, *128*, 13038–13039.
(31) Liberles, A.; Matlosz, B. *J. Org. Chem.* **1971**, *36*, 2710–2713.
(32) Schram, A. C.; Christenson, C. P. *Tex. J. Sci.* **1977**, *28*, 253–258.
(33) Weisz, A.; Andrzejewski, D.; Mandelbaum, A. *Org. Mass Spectrom.* **1992**, *27*, 891–895.
(34) Pavia, M. R.; Cohen, M. P.; Dilley, G. J.; Dubuc, G. R.; Durgin, T. L.; Forman, F. W.; Hediger, M. E.; Milot, G.; Powers, T. S.; Sucholeiki, I.; Zhou, S.; Hangauer, D. G. *Bioorg. Med. Chem.* **1996**, *4*, 659–666.
(35) Benton, F. L.; Dillon, T. E. *J. Am. Chem. Soc.* **1942**, *64*, 1128–1129.
(36) McOmie, J. F. W.; Watts, M. L.; West, D. E. *Tetrahedron* **1968**, *24*, 2289–2292.
(37) Nenov, S.; Clark, C. G., Jr.; Klapper, M.; Müllen, K. *Macromol. Chem. Phys.* **2007**, *208*, 1362–1369.

and methanol (225 mL) was added dropwise to a solution of 3,5-bis(4-toluenesulfonyloxy)iodobenzene (**3**) (23.3 g, 42.8 mmol) in methanol (100 mL) at 35 °C in a 1-L Erlenmeyer flask. The reaction mixture was stirred until 3,5-bis(4-toluenesulfonyloxy)iodobenzene was no longer visible by TLC (30 min). The reaction mixture was heated to 45 °C for an additional 15 min, cooled to room temperature, and diluted with water (to 800 mL). The reaction mixture was neutralized with HCl (5%, aq) and kept at 4 °C for 2 days. The precipitate was filtered, dissolved in diethyl ether, and extracted in sodium hydroxide (10%, aq). An oil separated, which was isolated, washed with water and diethyl ether, neutralized with HCl (5%, aq), extracted with diethyl ether, dried over $MgSO_4$, filtered, and concentrated in vacuo to yield a white solid (14.26 g, 85.4%). R_f (25% ethyl acetate/hexane) = 0.40. ^{1}H NMR (300 MHz, acetone-d_6, 20 °C): δ 2.47 (s, 3H, PhCH_3), 6.54 (s, H, Ar*H*), 6.87 (s, H, Ar*H*), 7.17 (s, H, Ar*H*), 7.49 (d, 2H, $^3J_{HH}$ = 8.1 Hz, CH_3Ar*H*), 7.77 (d, 2H, $^3J_{HH}$ = 8.4 Hz, CH_3Ar*H*), 9.11 (s, H, O*H*) ppm; ^{13}C NMR (75 MHz, acetone-d_6, 20 °C): δ 21.68, 93.76, 110.47, 123.22, 124.42, 129.38, 130.99, 133.11, 146.99, 151.50, 159.87 ppm; FDMS: *m*/*z* [ue^{-1}] 390.0 (100%), [M$^+$]; calcd, 389.9. Anal. Calcd for $C_{13}H_{11}IO_4S$: C, 40.02; H, 2.84; S, 8.22. Found: C, 40.15; H, 3.02; S, 8.12.

3-(4-Toluenesulfonyloxy)-5-dodecyloxyiodobenzene (5). A solution of 3-(4-toluenesulfonyloxy)-5-hydroxyiodobenzene (**4**) (14.26 g, 36.55 mmol), dodecanol (7.49 g, 40.20 mmol), and triphenylphosphine (11.98, 45.68 mmol) in THF (37 mL) was cooled to 0 °C in a 250-mL one-neck round-bottom flask, and a solution of diethyl azodicarboxylate (DEAD) (8.63 mL, 9.54 g, 54.82 mmol) in THF (74 mL) was added dropwise. The flask was closed with a stopper, allowed to warm to room temperature, and stirred for 15 h. The remaining DEAD was quenched with water, and the solvent was removed in vacuo. The reaction mixture was extracted with diethyl ether, washed with water, sodium hydroxide (5%, aq, 2×), hydrochloric acid (5%, aq), and water, dried over $MgSO_4$, filtered, and concentrated in vacuo, and recrystallized from methanol (120 mL) at 4 °C to yield white crystals (18.01, 88.2%). R_f (10% ethyl acetate/hexane) = 0.50. R_f (25% ethyl acetate/hexane) = 0.90. ^{1}H NMR (300 MHz, acetone-d_6, 20 °C): δ 0.88 (t, 3H, $^3J_{HH}$ = 6.9 Hz, CH_3), 1.20−1.50 (m, 18H, CH_2), 1.71 (quintet, 2H, $^3J_{HH}$ = 6.6 Hz, OCH$_2$CH_2), 2.47 (s, 3H, PhCH_3), 3.91 (t, 2H, $^3J_{HH}$ = 6.6 Hz, OCH_2), 6.58 (t, H, $^4J_{HH}$ = 2.1 Hz, Ar*H*), 6.96 (dd, H, $^4J_{HH}$ = 1.5, 2.1 Hz, Ar*H*), 7.23 (dd, H, $^4J_{HH}$ = 1.4, 2.2 Hz, Ar*H*), 7.50 (d, 2H, $^3J_{HH}$ = 7.8 Hz, CH_3Ar*H*), 7.77 (d, 2H, $^3J_{HH}$ = 8.4 Hz, CH_3Ar*H*) ppm; ^{13}C NMR (75 MHz, acetone-d_6, 20 °C): δ 14.46, 21.71, 23.41, 26.63, 30.06, 30.37, 30.39, 30.46, 32.71, 69.49, 93.81, 109.69, 123.64, 124.15, 129.47, 131.01, 133.07, 147.03, 151.44, 161.40 ppm; FDMS: *m*/*z* [ue^{-1}] 557.0 (100%), [M$^+$]; calcd, 558.1. Anal. Calcd for $C_{25}H_{35}IO_4S$: C, 53.76; H, 6.32; S, 5.74. Found: C, 53.81; H, 6.34; S, 5.56.

3-Dodecyloxy-5-hydroxyiodobenzene (6). Solutions of 3-(4-toluenesulfonyloxy)-5-dodecyloxyiodobenzene (**5**) (18.01 g, 32.20 mmol) in *tert*-butanol (17 mL) and sodium hydroxide (3.44 g, 86.10 mmol) in water (17 mL) were degassed by bubbling with argon for 5 min. The alkaline solution was added to the organic solution, and the bubbling was continued for 15 min. The reaction mixture was heated at reflux under argon overnight, cooled to room temperature, neutralized with hydrochloric acid (5%, aq), and extracted with diethyl ether. The ether solution was washed with brine, concentrated in vacuo to yield a colorless oil (12.69 g, 97.3%), which crystallized on standing and was used without further purification. R_f (10% ethyl acetate/hexane) = 0.15. R_f (15% ethyl acetate/hexane) = 0.59. R_f (25% ethyl acetate/hexane) = 0.68. For analytical purposes, column chromatography on silica gel using 25% ethyl acetate/hexane as eluent could be employed. ^{1}H NMR (300 MHz, acetone-d_6, 20 °C): δ 0.88 (t, 3H, $^3J_{HH}$ = 6.9 Hz, CH_3), 1.22−1.52 (m, 18H, CH_2), 1.74 (quintet, 2H, $^3J_{HH}$ = 6.3 Hz, OCH$_2$CH_2), 3.94 (t, 2H, $^3J_{HH}$ = 6.4 Hz, OCH_2), 6.41 (t, H, $^4J_{HH}$ = 2.1 Hz, Ar*H*), 6.78 (dd, H, $^4J_{HH}$ = 1.2, 2.0 Hz, Ar*H*), 6.82 (dd, H, $^4J_{HH}$ = 1.5, 1.8 Hz, Ar*H*), 8.63 (s, H, O*H*) ppm; ^{13}C NMR (75 MHz, acetone-d_6, 20 °C): δ 14.45, 23.42, 26.77, 30.15, 30.41, 30.47, 32.72, 68.88, 94.59, 102.83, 116.13, 118.01, 160.14, 162.03 ppm; FDMS: *m*/*z* [ue^{-1}] 404.7 (100%), [M$^+$]; calcd, 404.1. Anal. Calcd for $C_{18}H_{29}IO_2$: C, 53.47; H, 7.23. Found: C, 53.52; H, 7.24.

3-Dodecyloxy-5-hydroxyphenylethynyltrimethylsilane (7). 3-Dodecyloxy-5-hydroxyiodobenzene (**6**) (6.66 g, 16.46 mmol), copper iodide (0.42 g, 2.20 mmol), triphenylphosphine (0.302 g, 1.15 mmol), triethylamine (4.63 mL, 3.33 g, 32.92 mmol), and DMF (50 mL) were sparged with argon for 25 min in a 100-mL one-neck round-bottom flask. Ethynyltrimethylsilane (3.5 mL, 2.42 g, 24.69 mmol) was added, and argon was bubbled for an additional 5 min. Dichlorobis(triphenylphosphine)palladium(II) (0.404 g, 0.58 mmol) was added, and the flask was sealed with a stopper and stirred at room temperature for 2.5 days. The reaction mixture was concentrated in vacuo, extracted with diethyl ether, washed with water and hydrochloric acid (5%, aq), washed again with water, dried over $MgSO_4$, filtered, and concentrated in vacuo. The oil was chromatographed on silica gel using 20% ethyl acetate/hexane as eluent to yield a colorless oil (5.10 g, 82.6%). R_f (15% ethyl acetate/hexane) = 0.57. ^{1}H NMR (300 MHz, acetone-d_6, 20 °C): δ −0.22 (s, 9H, Si(CH_3)$_3$) 0.88 (t, 3H, $^3J_{HH}$ = 6.9 Hz, CH_3), 1.22−1.52 (m, 18H, CH_2), 1.74 (quintet, 2H, $^3J_{HH}$ = 6.6 Hz, OCH$_2$CH_2), 3.95 (t, 2H, $^3J_{HH}$ = 6.6 Hz, OCH_2), 6.43 (t, H, $^4J_{HH}$ = 2.2 Hz, Ar*H*), 6.49 (dd, H, $^4J_{HH}$ = 1.2, 2.2 Hz, Ar*H*), 6.52 (dd, H, $^4J_{HH}$ = 1.2, 2.2 Hz, Ar*H*), 8.52 (s, H, O*H*) ppm; ^{13}C NMR (75 MHz, acetone-d_6, 20 °C): δ 0.09, 14.45, 23.41, 26.80, 30.01, 30.41, 30.47, 32.72, 68.74, 93.49, 104.33, 106.30, 109.85, 112.03, 125.29, 159.33, 161.34 ppm; FDMS: *m*/*z* [ue^{-1}] 375.3 (100%), [M$^+$]; calcd, 374.3 ($C_{23}H_{38}O_2Si$).

3-Dodecyloxy-5-hydroxyphenylethyne (8). Solutions of 3-dodecyloxy-5-hydroxyphenylethynyltrimethylsilane (**7**) (5.00 g, 13.35 mmol) in THF (27 mL) and tetrabutylammonium fluoride trihydrate (5.05 g, 16.02 mmol) in THF (27 mL) were degassed by bubbling with argon for 15 min and cooled to 0 °C. The fluoride solution was added at once to the trimethylsilane (**7**) solution and stirred for 20 min at 0 °C. The reaction mixture was quenched with water, extracted with diethyl ether, washed with water and hydrochloric acid (5%, aq), washed again with water, dried over $MgSO_4$, filtered, and concentrated in vacuo to yield a pale yellow waxy solid (3.66 g, 90.6%). R_f (15% ethyl acetate/hexane) = 0.43. ^{1}H NMR (300 MHz, acetone-d_6, 20 °C): δ 0.88 (t, 3H, $^3J_{HH}$ = 6.9 Hz, CH_3), 1.22−1.52 (m, 18H, CH_2), 1.75 (quintet, 2H, $^3J_{HH}$ = 6.3 Hz, OCH$_2$CH_2), 3.55 (s, H, C≡C−*H*), 3.95 (t, 2H, $^3J_{HH}$ = 6.4 Hz, OCH_2), 6.45 (t, H, $^4J_{HH}$ = 2.2 Hz, Ar*H*), 6.53 (dd, H, $^4J_{HH}$ = 1.2, 2.2 Hz, Ar*H*), 6.55 (dd, H, $^4J_{HH}$ = 1.2, 2.1 Hz, Ar*H*), 8.55 (s, H, O*H*) ppm; ^{13}C NMR (75 MHz, acetone-d_6, 20 °C): δ 14.44, 23.41, 26.81, 30.00, 30.41, 30.46, 32.72, 68.75, 78.33, 84.44, 104.26, 110.16, 112.17, 124.54, 159.39, 161.38 ppm; FDMS: *m*/*z* [ue^{-1}] 303.3 (100%), [M$^+$]; calcd, 302.2. Anal. Calcd for $C_{20}H_{30}O_2$: C, 79.42; H, 10.00. Found: C, 79.46; H, 9.89.

Bis(3-dodecyloxy-5-hydroxyphenyl)ethyne (9). 3-Dodecyloxy-5-hydroxyphenylethyne (**8**) (1.00 g, 3.31 mmol), 3-dodecyloxy-5-hydroxyiodobenzene (**6**) (1.34 g, 3.31 mmol), copper iodide (0.084 g, 0.44 mmol), triphenylphosphine (0.061 g, 0.23 mmol), triethylamine (1.85 mL, 1.33 g, 13.22 mmol), and DMF (10 mL) were sparged with argon for 30 min in a 25-mL one-neck round-bottom flask. Dichlorobis(triphenylphosphine)palladium(II) (0.081 g, 0.12 mmol) was added, and the flask was sealed with a stopper and stirred at room temperature for 3 days. Diethyl ether and hydrochloric acid (5%, aq) were added to the reaction mixture, which was allowed to stir for 1 h. The ether layer was dried over $MgSO_4$ and adsorbed to silica gel (5.1 g) and loaded onto a silica gel column prepacked with 28% ethyl acetate/hexane and subsequently eluted to yield, after evaporation of solvent, a beige solid (1.74 g, 91.3%). R_f (30% ethyl acetate/hexane) = 0.60. ^{1}H NMR (300 MHz, acetone-d_6, 20 °C): δ 0.88 (t, 6H, $^3J_{HH}$ = 6.9 Hz, CH_3), 1.23−1.53 (m, 36H, CH_2), 1.76 (quintet, 4H, $^3J_{HH}$ = 6.6 Hz, OCH$_2$CH_2), 3.97 (t, 4H, $^3J_{HH}$ = 6.4 Hz, OCH_2), 6.45 (t, 2H, $^4J_{HH}$ = 2.2 Hz, Ar*H*), 6.59 (m, 4H, Ar*H*), 8.58 (s, 2H, O*H*) ppm; ^{13}C NMR (75 MHz, acetone-d_6, 20 °C): δ 14.46, 23.42, 26.83, 30.04, 30.45, 30.48, 32.73, 68.74,

Scheme 1. Synthesis of Biphasics **1** and **2**[a]

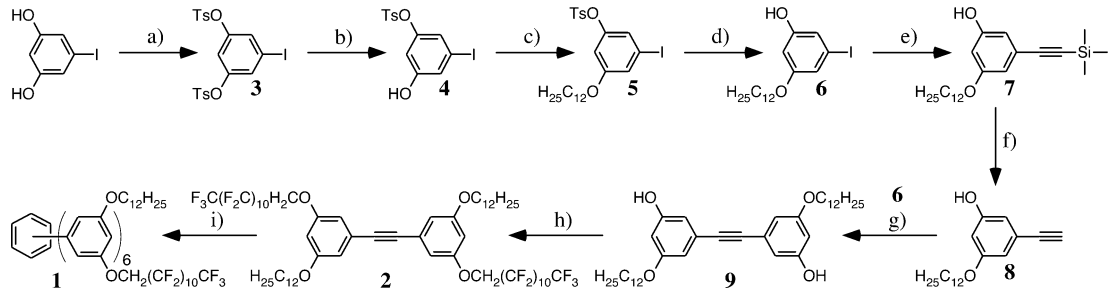

[a] (a) *p*-Toluenesulfonylchloride, pyridine, 25 °C, 5.5 d, 83.0%; (b) potassium hydroxide, water, methanol, 35 °C, 30 min, 45 °C, 15 min, 85.4%; (c) PPh_3, DEAD, THF, 0−25 °C, 15 h, 88.2%; (d) *t*-butanol, sodium hydroxide, water, reflux, 12 h, 97.3%; (e) ethynyltrimethylsilane, $Cl_2Pd(PPh_3)_2$, PPh_3, CuI, triethylamine, DMF, 25 °C, 2.5 d, 82.6%; (f) *t*-butyl ammonium fluoride trihydrate, THF, 0 °C, 25 min, 90.6%; (g) 3-dodecyloxy-5-hydroxyiodobenzene (**6**), $Cl_2Pd(PPh_3)_2$, PPh_3, CuI, triethylamine, DMF, 25 °C, 3 d, 91.3%; (h) Cs_2CO_3, DMF, 1-perfluoroundecylmethylnonaflate, 65 °C, 1.5 d, 85.2%; (i) $Co_2(CO)_8$, dioxane, sealed tube, 160 °C, microwave reactor, 4 h, repeated three times (the solution was diluted, and the quantity of catalyst successively halved for each repetition), 92.7%.

89.52, 104.01, 109.68, 111.76, 125.35, 159.42, 161.41 ppm; FDMS: *m*/*z* [ue^{-1}] 578.5 (100%), [M$^+$]; calcd, 578.4. Anal. Calcd for $C_{38}H_{58}O_4$: C, 78.85; H, 10.10. Found: C, 77.31; H, 9.91.

Bis(3-(1-perfluoroundecylmethoxy)-5-dodecyloxyphenyl)ethyne (2). A mixture of bis(3-dodecyloxy-5-hydroxyphenyl)ethyne (**9**) (0.5 g, 0.86 mmol) and 1-perfluoroundecylmethylnonaflate (3.2 g, 3.63 mmol) in DMF (33 mL) was degassed by bubbling with argon for 25 min. Cesium carbonate (2.4 g, 7.37 mmol) was added, and the reaction mixture was heated to 65 °C for 1.5 days. The reaction mixture was concentrated in vacuo and dissolved in refluxing ethyl acetate in water. The aqueous layer was extracted a second time with refluxing ethyl acetate. The organic layers were combined and filtered and concentrated in vacuo. The powder was filtered with refluxing hexane to remove the excess nonaflate and concentrated in vacuo to yield a white powder (1.28 g, 85.2%). R_f (5% ethyl acetate/hexane) = 0.76. ^{1}H NMR (700 MHz, $C_2D_2Cl_4$, 120 °C): δ 0.97 (t, 6H, $^3J_{HH}$ = 7.0 Hz, C*H*$_3$), 1.32−1.48 (m, 32 H), 1.54 (quintet, 4H, $^3J_{HH}$ = 7.0 Hz, OCH$_2$CH$_2$C*H*$_2$), 1.85 (quintet, 4H, $^3J_{HH}$ = 7.0 Hz, OCH$_2$C*H*$_2$), 4.05 (t, 4H, $^3J_{HH}$ = 7.0 Hz, OC*H*$_2$CH$_2$), 4.53 (t, 4H, $^3J_{HF}$ = 13.0 Hz, OC*H*$_2$CF$_2$), 6.60 (s, 2H, $^4J_{HH}$ = 2.1 Hz, 4′-Ar*H*), 6.78 (s, 2H, Ar*H*), 6.86 (s, 2H, Ar*H*) ppm; ^{13}C NMR (175 MHz, $C_2D_2Cl_4$, 120 °C): δ 13.52, 22.25, 25.76, 28.93, 29.03, 29.21, 29.24, 29.28, 29.30, 31.57, 65.99 (t, $^2J_{CF}$ = 27.1 Hz), 68.77, 89.01, 104.06, 110.65, 112.73, 124.79, 158.51, 160.44 ppm; FDMS: *m*/*z* [ue^{-1}] 1742.0 (100%), [M$^+$]; calcd, 1742.4. Anal. Calcd for $C_{62}H_{60}F_{46}O_4$: C, 42.72; H, 3.47. Found: C, 41.53; H, 3.14.

Hexakis(3-(1-perfluoroundecylmethoxy)-5-dodecyloxyphenyl)-benzene (1). Dicobalt octacarbonyl (2.0 mg, 0.006 mmol) was added to a 10-mL glass microwave reaction vessel (CEM) charged with bis(3-(1-perfluoroundecylmethoxy)-5-dodecyloxyphenyl)ethyne (**2**) (200 mg, 0.12 mmol), 1,4-dioxane (1.15 mL, degassed), and a magnetic stir bar. The reaction mixture was allowed to stir under a slow stream of argon and heated gently to 100 °C for 2 min. The vessel was sealed with a cap with an integrated septum for measuring the internal pressure (Intellivent, CEM) and heated to 160 °C for 4 h. The reaction mixture was cooled to room temperature and diluted with dioxane (1.15 mL). A fresh quantity of dicobalt octacarbonyl (2.0 mg, 0.006 mmol) was added, and the reaction was continued at 160 °C for 4 h. The catalyst replenishment, dilution, and reaction procedures were repeated. The mixture was extracted with hot ethyl acetate, washed with HCl (5%, aq) and water, dried over $MgSO_4$, and filtered. The solution was concentrated in vacuo, dissolved in hot 5% ethyl acetate in hexane, and chromatographed on silica gel at room temperature, using the same solvent as eluent. The solvent was evaporated to yield a pale yellow, waxy solid. The solid was dissolved in hot acetone and precipitated on cooling to give a white powder (230 mg, 92.7%). R_f (5% ethyl acetate/hexane) = 0.69. ^{1}H NMR (500 MHz, $C_2D_2Cl_4$, 137 °C): δ 0.96 (t, 18H, $^3J_{HH}$ = 7.0 Hz, C*H*$_3$), 1.31−1.46 (m, 108H, C*H*$_2$), 1.63 (quintet, 12H, $^3J_{HH}$ = 6.8 Hz, OCH$_2$C*H*$_2$), 3.70 (t, 12H, $^3J_{HH}$ = 6.5 Hz, OC*H*$_2$CH$_2$), 4.11 (t, 12H, $^3J_{HF}$ = 13.0 Hz, OC*H*$_2$CF$_2$), 6.20 (s, 6H, Ar*H*), 6.23 (t, 6H, $^4J_{HH}$ = 2.2 Hz, 4′-Ar*H*), 6.29 (s, 6H, Ar*H*) ppm; ^{13}C NMR (125 MHz, $C_2D_2Cl_4$, 137 °C): δ 13.29, 22.13, 25.63, 28.85, 28.90, 28.93, 29.15, 29.20, 29.25, 29.31, 31.49, 66.32 (t, $^2J_{CF}$ = 27.1 Hz), 68.79, 102.26, 111.15, 113.10, 139.57, 142.14, 157.95, 159.60 ppm; ^{19}F NMR (470 MHz, $C_2D_2Cl_4$, 137 °C): δ −80.28 (3F, C*F*$_3$), −118.28 (2F, CH$_2$C*F*$_2$), −120.15 (8F, C*F*$_2$), −120.40 (4F, C*F*$_2$), −121.23 (2F, C*F*$_2$), −121.96 (2F, C*F*$_2$), −124.62 (2F, C*F*$_2$CF$_3$) ppm; MALDI (TCNQ): *m*/*z* [ue^{-1}] 5229 (100%), [M$^+$]; calcd, 5227. Anal. Calcd for $C_{186}H_{180}F_{138}O_{12}$: C, 42.72; H, 3.47. Found: C, 43.82; H, 3.64.

Results and Discussion

For the synthesis of a biphasic HPB amphiphile (**1**), three criteria were considered: (1) A moderate barrier to phenylbenzene rotation[38,39] (to enable the conformation to be dictated by phase separation of hydrocarbon and fluorocarbon chains with the possibility of internal rotation) suggested meta substitution of the phenyl rings, ideal for the lateral packing of such chains, (2) the conventional difficulty of handling and purification of fluorous materials, and (3) the desymmetrization of the resorcinol-based building blocks such that a single HPB isomer with one hydrocarbon and one fluorocarbon on each phenyl ring is formed. To accomplish this, a general route of sequential alkylation of the two phenols of a substituted resorcinol during the buildup of a biphasic diphenylacetylene (**2**), a precursor to the HPB (**1**), was followed (Scheme 1). Specifically, 3-(4-toluenesulfonyloxy)-5-hydroxyiodobenzene (**4**) was generated by the selective alkaline monohydrolysis[40] of the bistosylate **3** of 5-iodoresorcinol.[32−36] This has the second advantage that the sodium salt of the product, **4**, is an oil that separates from the diethyl ether and aqueous solutions, which retain all other reaction products. Upon neutralization of the oil, the product was received analytically pure without chromatography. Mitsunobu etherification of the phenol with dodecanol introduced the hydrocarbon chain into 3-(4-toluenesulfonyloxy)-5-dodecyloxyiodobenzene (**5**). Hydrolysis of the remaining tosylate provided phenol **6**, which was tolerated by the palladium-catalyzed Hagihara−Sonogashira reaction[41] of the iodide with trimethylsilylacetylene to furnish 3-dodecyloxy-5-hydroxyphe-

(38) Gust, D.; Patton, A. *J. Am. Chem. Soc.* **1978**, *100*, 8175–8181.
(39) Pepermans, H.; Willem, R.; Gielen, M.; Hoogzand, C. *Magn. Reson. Chem.* **1988**, *26*, 311–318.
(40) Kampouris, E. M. *J. Chem. Soc.* **1965**, 2651–2654.
(41) Sonogashira, K.; Tohda, Y.; Hagihara, N. *Tetrahedron Lett.* **1975**, *16*, 4467–4470.

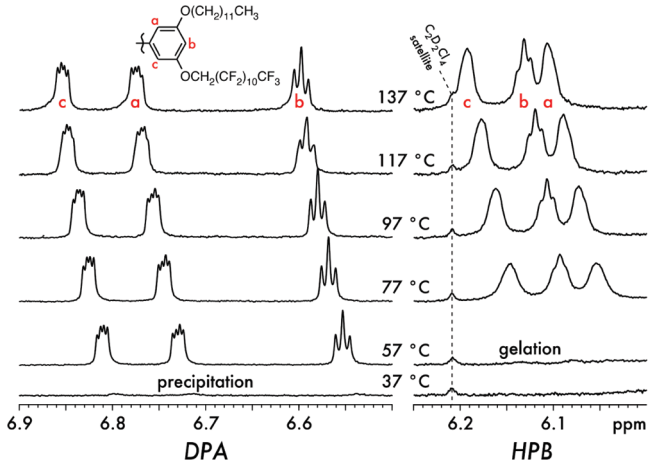

Figure 2. Temperature-dependent ^{1}H NMR aryl resonances (300 MHz, $C_2D_2Cl_4$) of the biphasic DPA (**2**) and HPB (**1**).

nylethynyltrimethylsilane (**7**) after column chromatography. Cleavage of the trimethylsilyl group gave ethyne **8**, and an additional Hagihara−Sonogashira reaction with 3-dodecyloxy-5-hydroxyiodobenzene (**6**) yielded diphenylacetylene **9** with two remaining phenols, readily purified by column chromatography. The phenols were directly etherified[42−44] with cesium carbonate and 1-perfluoroundecylmethylnonaflate[37] at 65 °C to afford the biphasic DPA (**2**), which was purified by washing with water and a series of organic solvents, and finally extracted with hot hexane. DPA **2** was quantitatively cyclotrimerized using dicobalt octacarbonyl[45,46] in dioxane at 160 °C under microwave irradiation in three cycles with catalyst replenishment and successive dilution of the reaction medium. Hexakis(3-(1-perfluoroundecylmethoxy)-5-dodecyloxyphenyl)benzene (**1**), when dissolved in an organic solvent such as hexane, THF, benzene, or toluene, formed gels at high concentration. Unlike DPA **2**, the biphasic HPB (**1**) could be chromatographed on silica gel using a hexane−ethyl acetate mixture as eluent, which dissolved completely the HPB at high concentration at room temperature. NMR spectra were obtained at elevated temperature because of aggregation in most solvents. The highly symmetric structures of both DPA **2** and HPB **1** are reflected in the ^{1}H NMR spectra (Supporting Information) with three aromatic resonances mutually coupled to the other meta protons (Figure 2). The peak widths of the aryl resonances are appreciably narrower for the DPA (**2**) over a broad temperature range, which indicates the significantly lower mobility of the HPB (**1**), most likely due to the slower flip (180° rotation) rate of the phenyl rings. The ^{13}C and ^{19}F NMR spectra (Supporting Information) are as expected[42,44] for the 1-perfluoroundecylmethyl aryl ether with well-separated CF_3 and CF_2 regions.

DSC was performed for DPA **2** and HPB **1** (Figure 3). The melting point of the HPB (**1**) (86 °C) is similar to that for fluorocarbon melting, as reported for the SFA, perfluoro(dodecyl)dodecane (**F12H12**).[12,13] The melting point of the DPA (**2**) is much higher (123 °C), presumably due to the more dense chain packing as well as the intermolecular π-stacking, not possible in the HPB.

To gain a better understanding of the phase transformations and of the associated length scales, X-ray scattering, at small- (SAXS), mid- (MAXS), and wide- (WAXS) angles, was employed from oriented fibers as a function of temperature. The SAXS, MAXS, and WAXS images show equatorial reflections in SAXS and a set of equatorial reflections together with a prominent meridional reflection in WAXS. The former gives rise to a lamellar periodicity of 3.9 and 6.6 nm for HPB (**1**) and DPA (**2**), respectively, with lamellar orientations *parallel* to the fiber axis (Figure 4). The 3.9-nm periodicity for HPB **1** roughly corresponds to a fully extended, single molecular length, and the 6.6-nm periodicity for DPA **2** is a supramolecular distance. The strong meridional WAXS reflection with a *d*-spacing of 0.5 nm reflects the van der Waals distances between adjacent chains *along* the fiber axis. A second, albeit less intense, reflection, with a distance of 0.44 nm, in the WAXS curve of DPA **1** is likely due to correlations between adjacent hydrocarbon chains. These correlations become weaker/broader in the HPB **2** case. The packing behavior of DPA **2** is as anticipated (Figure 5). The two rigid fluorocarbons pack laterally with the fluorocarbon chains of adjacent molecules (WAXS, meridional axis). If the packing within a layer is made in a parallel fashion, this enables the efficient packing and phase separation of all three components: fluorocarbon, hydrocarbon, and the diphenylacetylene core. As a consequence, the fluorocarbons form bilayers, typical for fluorous biphasic materials[12,14] with sufficient driving force for phase separation, and are not likely to be tilted significantly because of the perfect packing distances set up by the chemical placement of the chains on the DPA core. On the other hand, the hydrocarbon chain from each layer does not form a fully extended bilayer and is either partially interdigitated or tilted because of the lower density, afforded by the larger fluorocarbon-radius-determined packing.[47] According to WAXS of HPB **1**, the lateral interchain spacing is similar to that of the DPA **2**, but the MAXS peak at 3.9 nm signifies a molecular lamellar spacing. In addition, a weak and broad *d*-spacing is observed at ca. 6.5 nm, in the same range as the main bilayer-derived *d*-spacing for DPA **2**. This feature suggests the presence of a second, however, minor structure. As will be discussed below, this corresponds to HPB **1** packed into fluorocarbon bilayer lamellae.

Solid-state NMR offers the opportunity to resolve ambiguities in the X-ray results, particularly in the absense of a single crystal. To understand better the differences in the lamellar spacings of the two biphasics, ^{19}F solid-state NMR experiments (Figure 6) were performed. The dependence of the chemical shift of the ^{19}F CF_3 resonance on the chemical environment (e.g., fluorocarbon, hydrocarbon, or mixed) has recently been mapped[48] and, combined with X-ray periodicities, enabled the elucidation of local packing topologies. The CF_3 chain ends of DPA **2** are clearly in fluorocarbon domains (Figure 6, top), consistent with the bilayer expectation from X-ray results. In stark contrast, the HPB CF_3 resonances are distributed among all three environments, and the majority is in mixed domains (Figure 6, middle). Annealing at the melting point increased the fraction of CF_3 resonances in the fluorocarbon domain, but

(42) Pensec, S.; Tournilhac, F. G.; Bassoul, P.; Durliat, C. *J. Phys. Chem. B* **1998**, *102*, 52–60.
(43) Sinou, D.; Pozzi, G.; Hope, E. G.; Stuart, A. M. *Tetrahedron Lett.* **1999**, *40*, 849–852.
(44) Sinou, D.; Maillard, D.; Pozzi, G. *Eur. J. Org. Chem.* **2002**, *2002*, 269–275.
(45) Krürke, U.; Hübel, W. *Chem. Ber.* **1961**, *64*, 2829–2856.
(46) Grotjahn, D. B. In *Comprehensive Organometallic Chemistry II*; Abel, E. W.; Stone, F. G. A.; Wilkinson, G.; Hegedus, L. S., Eds.; Pergamon: Oxford, 1995; Vol. 12, pp 741−770.
(47) Ku, C.-Y.; Lo Nostro, P.; Chen, S.-H. *J. Phys. Chem. B* **1997**, *101*, 908.
(48) Lee, Y. J.; Clark, C. G., Jr.; Graf, R.; Wagner, M.; Müllen, K.; Spiess, H. W. *J. Phys. Chem. B* **2009**, *113*, 1360–1366.

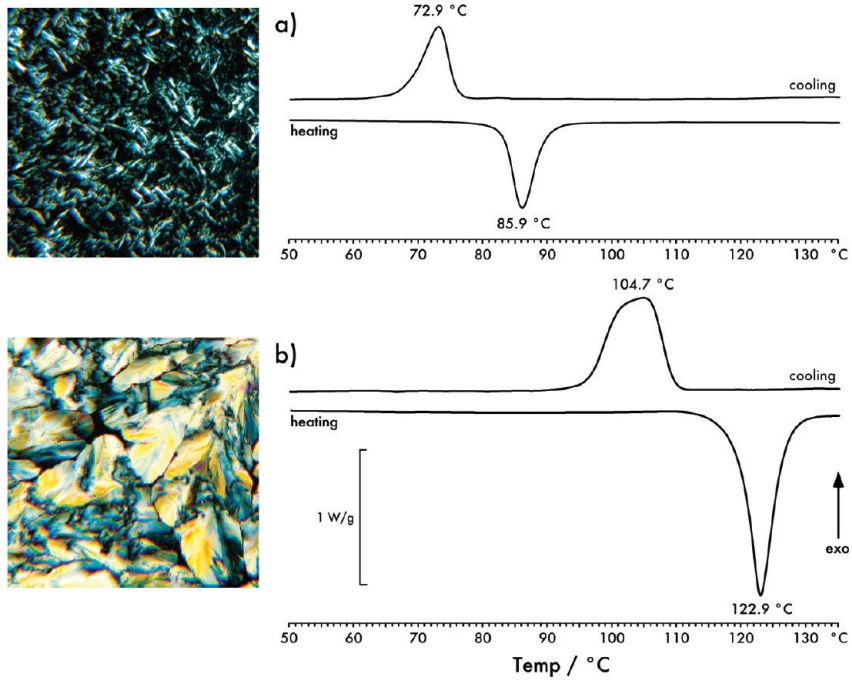

Figure 3. Polarized optical micrographs, obtained at room temperature after cooling from an isotropic melt at 1 °C/min, and DSC of (a) the biphasic HPB (**1**) and (b) the biphasic DPA (**2**).

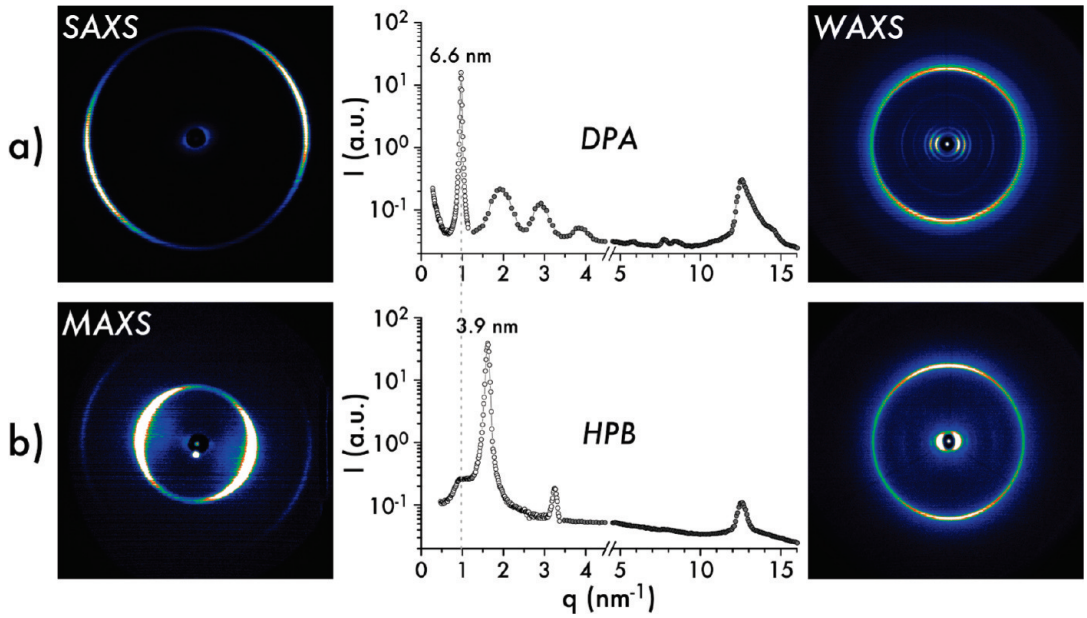

Figure 4. X-ray scattering, SAXS or MAXS (open circles) where appropriate and WAXS (filled circles), results of extruded fibers of the (a) the biphasic DPA (**2**) and (b) the biphasic HPB (**1**).

nevertheless, the majority of chains remained in mixed domains (Figure 6, bottom). Furthermore, cross-peaks in the 2-D ^{19}F exchange experiment using radio frequency-driven dipolar recoupling[49,50] (RFDR) (Figure 7), which probes chemical shift correlation in a few nanometers length scale, show that CF_3 groups in the different environments are in close spatial proximity to one another. This demonstrates conclusively that the hydrocarbon and fluorocarbon side chains are mixed within a single layer and even within a single HPB molecule. The observed lamellar order in this context is somewhat surprising: not only are the immiscible chains mixed, but they are packed laterally (Figure 8).

Even if phase separation within a single layer is the dominant feature, the presence of a few chains of different type may be enough to lose correlation between fluorocarbon layers (because of the smaller interfacial area between layers, compared to the lateral, interstitial surface area between chains) and give a mixed lamella (Figure 8a). Since the chains of different type are incompatible, they must be kinetically trapped. This can be explained by several factors. (1) Both types of chains are rodlike

(49) Bennett, A. E.; Ok, J. H.; Griffin, R. G.; Vega, S. *J. Chem. Phys.* **1992**, *96*, 8624.
(50) Feike, M.; Graf, R.; Schnell, I.; Jäger, C.; Spiess, H. W. *J. Am. Chem. Soc.* **1996**, *118*, 9631.

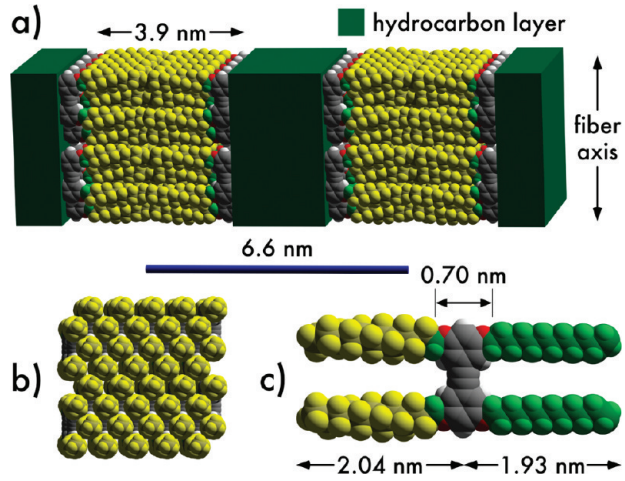

Figure 5. Proposed packing of the biphasic DPA (**2**). (a) Fluorocarbon bilayer lamellar packing, (b) fluorocarbon chain end (CF_3) view from a single molecular layer, and (c) DPA molecular dimensions.

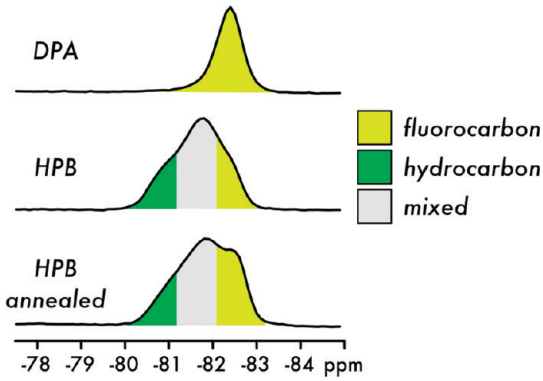

Figure 6. ^{19}F MAS NMR CF_3 chemical shift analysis of the local packing environment below all thermal transitions (55 °C). (a) The biphasic DPA (**2**), (b) the biphasic HPB (**1**), cooled from the isotropic melt at 10 °C/min, and (c) after annealing at 85 °C for 1 d.

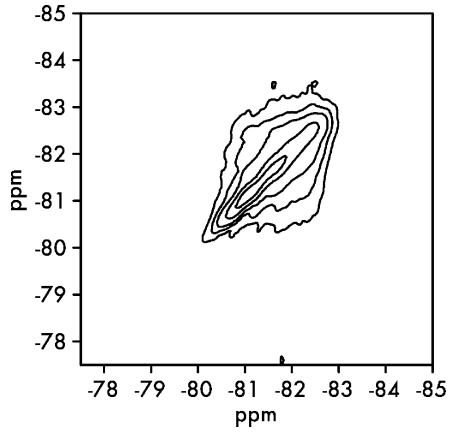

Figure 7. Two-dimensional ^{19}F exchange NMR spectrum using the RFDR scheme of the biphasic HPB (**1**) at 55 °C after annealing at 85 °C for 1 d.

when fully extended and of similar length, and they are shape compatible for packing. Thus, they fulfill van der Waals interactions but own a substantial mismatch in volume, such that mixing of the chains would give rise to a more homogeneous density profile. (2) Annealing clearly indicates an initially increased formation of the fluorocarbon bilayer (CF_3 in fluorocarbon environment). However, this did not change signifi-

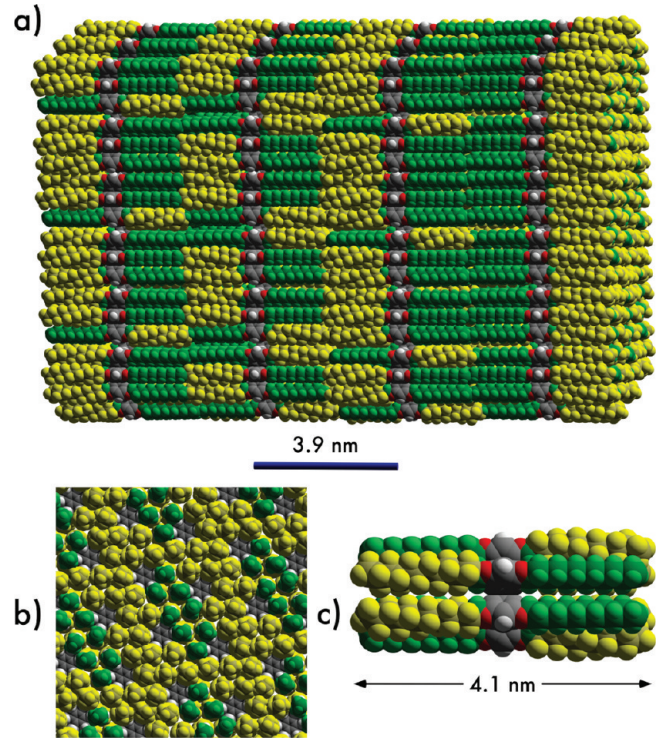

Figure 8. Proposed packing of the biphasic HPB (**1**). (a) Unilamellar mixed conformation packing, (b) chain end (CF_3) view from a single molecular layer, and (c) HPB molecular dimensions.

cantly with longer annealing time, which suggests that annealing increases the match in the local surface composition from intermolecular interactions (e.g., by an overall rotation of the molecule around its C6 symmetry axis, Figure 8b). Reinforcing this is the finding of comparable melting temperatures for the HPB (**1**) and the semifluorinated alkane, **F12H12**, with similar intermolecular interaction surfaces.[51] (3) The energetic barrier to rotation of an HPB phenyl group in solution is 15−20 kcal/mol.[38,39] Such barriers are expected to be higher in bulk, exacerbated by the conformations that the molecule must undergo in the presence of laterally interacting neighboring molecules. This is supported by the broad ^1H aryl resonances, even in solution NMR (Figure 2), for the biphasic HPB (**1**) in the relevant temperature range. Each of these factors taken together strongly suggests that the conversion between rotational isomers must be too slow to reach practically the thermodynamically preferred conformation.

Addition of only 1% of the DPA (**2**), which itself possesses the desired chain packing, to the HPB (**1**) gave two additional melting transitions at higher temperature (97.6 (minor), 110.3 °C), but lower than that of pure DPA **2** (Figure 9). This indicates the presence of two new structures, which are more stable than those of the mixed chain lamellae of pure HPB **1** or of **F12H12**. The HPB **1** and DPA **2** molecules cocrystallize and do not form a eutectic, more typical of defect-determined crystallization from binary mixtures. A crystal morphology above 100 °C, very different from that of pure HPB **1** and which takes several hours to grow, was observed by microscopy, consistent with a kinetically controlled process.

The X-ray measurements depicted in Figure 10 were obtained on cooling from 100 °C, following annealing at each temperature

(51) Nuñez, E.; Clark, C. G., Jr.; Cheng, W.; Best, A.; Floudas, G. A.; Semenov, A.; Fytas, G.; Müllen, K. *J. Phys. Chem. B* **2008**, *112*, 6542–6549.

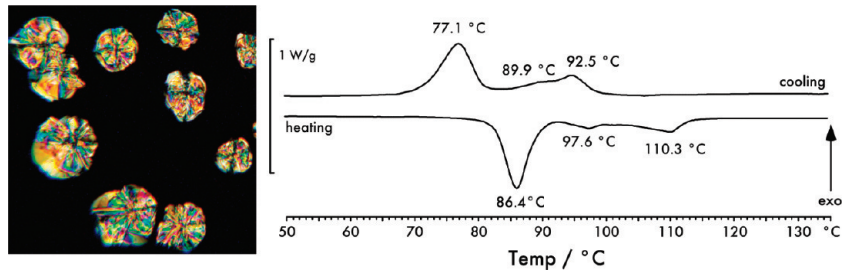

Figure 9. Polarized optical micrograph, obtained at 105 °C after cooling from an isotropic melt at 1 °C/min, and DSC of the biphasic HPB (**1**), doped with 1% of the biphasic DPA (**2**).

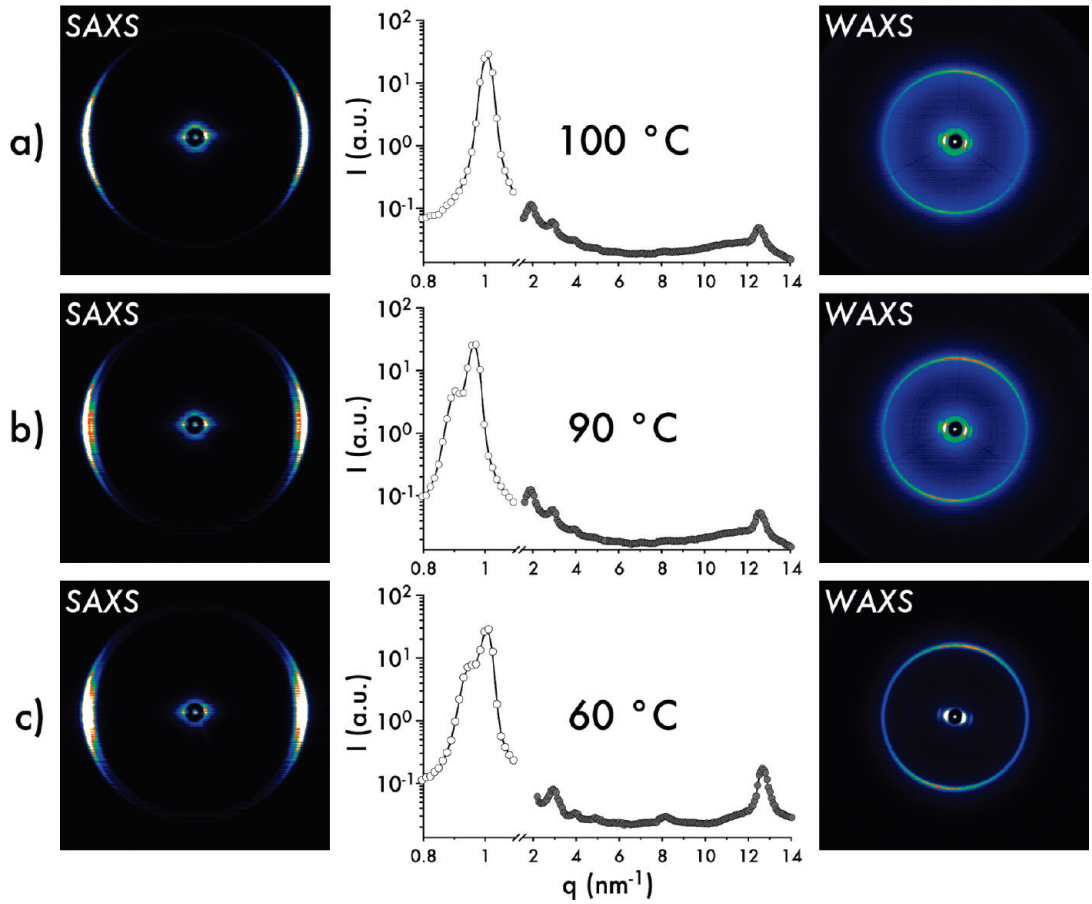

Figure 10. X-ray scattering (SAXS (open circles), WAXS (filled circles)) results of an extruded fiber of the 1% DPA-doped biphasic HPB (after annealing at 100 °C), **1**, at (a) 100, (b) 90, and (c) 60 °C, indicating the supramolecular (bilayer lamellar) *d*-spacings.

for 1 h. SAXS and WAXS (Figure 10b,c) of the 1% DPA (**2**)-doped HPB (**1**) confirmed that supramolecular lamellar packing resulted with *d*-spacings (6.5 and 7 nm below 90 °C) similar to that of DPA **2** and to the weak MAXS reflection present in undoped HPB **1**. Most prevalent at 100 °C (Figure 10a) was a single equatorial SAXS reflection with a spacing of 6.3 nm and corresponding higher-order WAXS reflections (i.e., with lamellar periodicity perpendicular to the fiber axis). The shorter distance is consistent with complete interdigitation of the hydrocarbon bilayer chains, made possible by the collective increase in molecular radius due to packing all of the fluorocarbon chains on one face.

^{19}F MAS NMR (Figure 11, Supporting Information) of the doped HPB showed that the majority of CF_3's are in fluorocarbon bilayers at 55 °C, but revealed a significant proportion remaining in mixed or hydrocarbon defect environments. Upon heating of the sample, monitoring the CF_3 resonances in situ (Figure 11) showed that the defect structures were the first to melt, corresponding to the lowest temperature endotherm in the DSC, and the fluorocarbon bilayer domain was the last to melt, corresponding to the highest temperature endotherm in the DSC. This, taken together with the X-ray results, indicates that only the fluorocarbon bilayer structure is stable above 90 °C.

The correlation between perfectly phase-separated material must then give higher contrast for X-ray scattering compared to that of the mixed conformations, as the X-ray showed no significant amount of the unimolecular lamellae, and all CF_3's are equally observed in the solid-state NMR experiment. This renders X-ray experiments much more sensitive to study the molecularly phase-separated material (Figure 12). In this context, the two *d*-spacings in SAXS likely correspond to different modes of hydrocarbon packing, which may be linked to the extent of axial registration of HPBs in a domain (columnar vs lamellar packing), but further evidence is needed. The lower density of

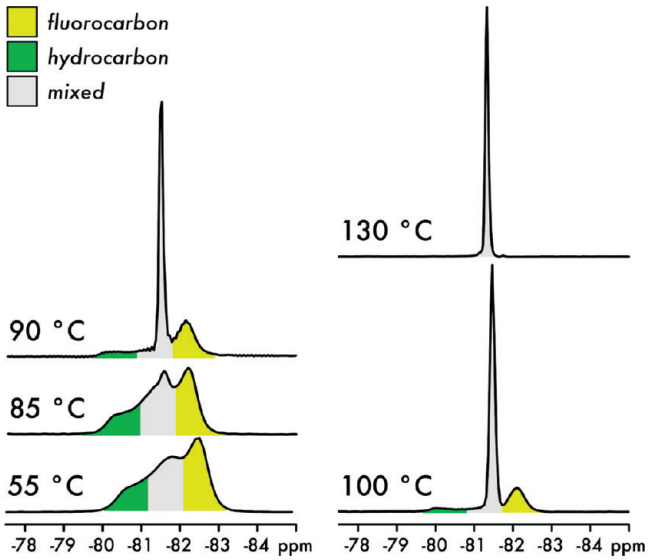

Figure 11. Temperature-dependent ^{19}F MAS NMR CF_3 chemical shift analysis of the local packing environment (fluorocarbon, hydrocarbon, or mixed) for the biphasic HPB (**1**), doped with 1% biphasic DPA (**2**), preannealed at 105 °C for 1 d.

packed chains (six vs seven chains for the same lateral packing area for the HPB (**1**) and DPA (**2**), respectively) and lack of π-contacts are responsible for the lower melting point of the respective bilayers with similar *d*-spacings. That the fluorocarbon bilayer with fully interdigitated hydrocarbon lamella is more thermally stable than the HPB (**1**) molecular lamellae and **F12H12** fluorocarbon bilayers indicates that the entropy has indeed been paid intramolecularly by the tethering of chains to the HPB, but requires nucleation centers made stable by the addition of DPA (**2**).

Summary and Conclusions

Biphasic (fluorocarbon/hydrocarbon) amphiphiles tethered to cores with only rotational degrees of freedom (phenylacetylene and phenylbenzene in DPA **2** and HPB **1**, respectively) were synthesized, and the bulk-phase self-assembly was studied. The strategy, which synthetically places chains on rigid cores at distances commensurate with their packing requirements, gives predictable thermodynamically driven self-assembly behavior if the barrier to rotation is low as in the biphasic DPA (**2**) case. Grafting at bulk density through intramolecular contacts, as in the HPB (**1**) case, requires that rotational dynamics be considered for efficient phase formation. Intramolecular interactions force incompatible segments into proximity if there is not sufficient conformational mobility, giving a kinetically trapped phase, stabilized by favorable interactions with neighboring molecules. The fluorocarbon bilayer thermodynamic equilibrium is reached in HPB **1** with the addition of traces of a stable nucleation center or seed (DPA, **2**) with a compatible lattice. DPA unlocks the kinetically frustrated conformations in HPB by promoting the interconversion between rotational isomers toward the thermodynamically favorable state. Investigation of the intrinsic conformational mobilities and dynamics (by employing the uncompensated C−F end dipole through dielectric spectroscopy) will be presented in a future report.[52]

(52) Elmahdy, M. M.; Floudas, G. A.; Clark, C. G., Jr.; Müllen, K. To be submitted for publication.

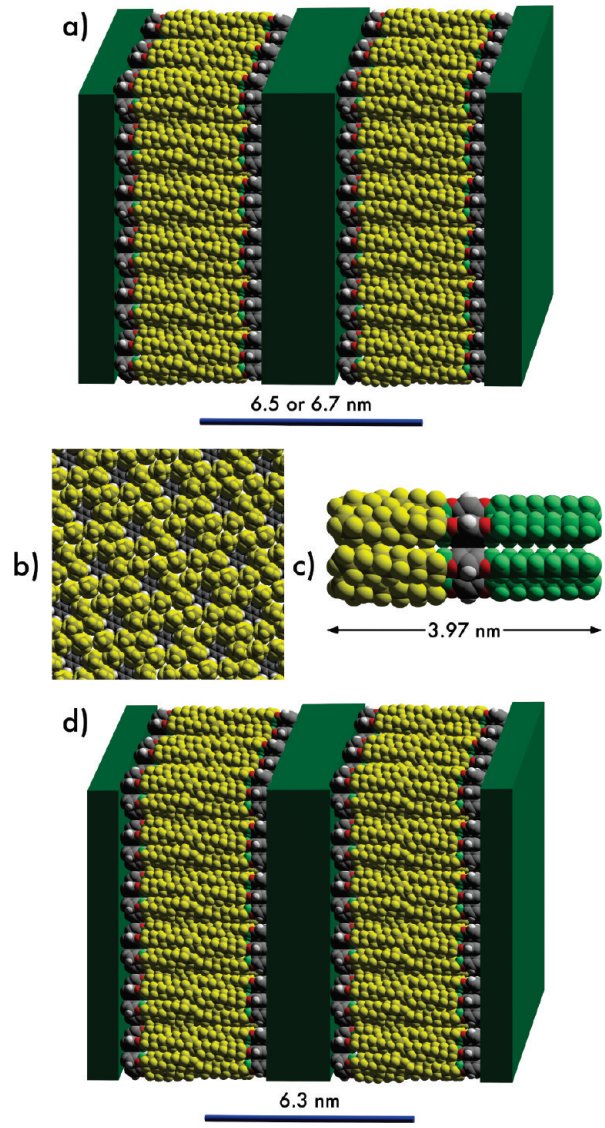

Figure 12. Proposed packing of the biphasic HPB (**1**), crystallized above 90 °C using 1% of the biphasic DPA (**2**). (a) Fluorocarbon bilayer lamellar packing at 55−90 °C, (b) fluorocarbon chain end (CF_3) view from a single molecular layer, (c) HPB molecular dimensions, and (d) proposed packing with full interdigitation of the hydrocarbon at 100 °C.

Molecularly tethered amphiphiles with a soft internal potential for rotation or with long-lived kinetically trapped states that allow for mixed fluorocarbon and hydrocarbon chains can provide films with a variety of different surface energies that depend on the degree of mixing. Such amphiphiles effectively generate films with a variety of surface energies giving rise to surfaces with controlled wetting properties. This would not be possible with simple SFAs, as overwhelming enthalpic interactions drive the system into the phase-separated state. Finally, a multiphasic HPB architecture should be a versatile platform for the construction of diverse and complex 3-D solid-state motifs from the high synthetic and supramolecular precision of lateral juxtaposition of both compatible and incompatible chains. This is especially promising, given the influential role of both intra- and intermolecular interactions, not available in traditional block copolymer amphiphiles.

Acknowledgment. The research was supported by the U.S. National Science Foundation (MPS-DRF, Award DMR-0207086),

the Deutsche Forschungsgemeinschaft (DFG) in the frame of the Sonderforschungsbereich (SFB) 625, and the Max Planck Society. We gratefully acknowledge this support. We thank S. Koynova and E. Deister for assistance with the DSC experiments, M. Bach for assistance with x-ray experiments, as well as S. Spang, P. Kindervater, and M. Wagner for assistance with solution-state NMR experiments.

Supporting Information Available: ^{1}H and ^{13}C solution NMR spectra for DPA **2** and HPB **1**, a ^{19}F solution NMR spectrum for HPB **1**, and temperature-dependent ^{1}H and ^{19}F MAS solid-state NMR spectra for HPB **1**. This material is available free of charge via the Internet at http://pubs.acs.org.

JA900999F